Velocity analysis of fluid structures from ballistic images in the near field of an aerated spray

D. L. Sedarsky *
Department of Physics, Lund University, Lund, Sweden
J. Gord, B. Kiel, C. Carter
Air Force Research Laboratory, Wright-Patterson AFB, USA
T. Meyer
Iowa State University, Ames, IA 50011, USA
M. A. Linne
Sandia National Laboratories, Livermore, CA 94551, USA

Abstract

This work presents an application of the diagnostic technique commonly known as ballistic imaging, which is adept at resolving internal structures in optically dense media. A time-gated imaging system specifically designed for transient fuel sprays was applied to a nitrogen aerated water jet issuing into ambient air. The images acquired by this system reveal fluid structures undergoing breakup in the near-nozzle region of the flow. To unambiguously describe the forces that act to break apart the liquid core in a spray, one must directly measure the force vectors themselves. To this end, obtaining velocity and acceleration data from near-field fluid features is essential to understanding spray breakup dynamics. By employing a fast-framing CMOS camera and a new ultrafast laser source, consecutive ballistic images with a temporal separation of 10 μs were acquired. This fast detection scheme allows the determination of velocity information from pairs of ballistic images using cross-correlation methods. Three approaches were applied to obtain velocity information: particle-tracking correlation analysis was applied to obtain velocity for small droplets resolved in the images, conventional non-adaptive grid correlation analysis was applied across the entire field-of-view, and image segmentation with subsequent grid correlation analysis was applied over the resolved fluid features larger than a reasonable size threshold. The results presented here are an important step in understanding how primary breakup occurs in dense sprays, and opens the way for analysis of spray breakup dynamics using time-resolved single-shot ballistic imaging.

Introduction

Liquid fuels are prevalent in combustion devices because they have higher energy densities than gaseous fuels and can be conveniently transported and stored. The principal difficulty in liquid-fuel combustion lies in controlling the fuel/air mixture fraction in a steadily reacting or cyclically reacting flow. To maximize combustion efficiency and minimize the production of pollutants such as soot and NO_x, it is necessary to rapidly disperse the fuel into the airstream using a spray. As a consequence, the fluid dynamics of spray breakup are directly coupled to mixture preparation, such that a detailed understanding of spray fluid dynamics is essential for the design of efficient and environmentally responsible combustion devices.

For many sprays, complete and non-invasive diagnostics of the flow is problematic due, first, to the sensitivity of the flow which renders probes or devices placed in the flow volume impractical, and second, to the high optical density of some regions of the flow, often termed the "near-field" or "dense spray" region. These dense portions of the spray frustrate most optical diagnostics due to the large degree of scattering exhibited by these regions. Ballistic imaging (BI) is an optical technique designed to mitigate the interference from scattered light to form high-resolution shadowgram-type images of structures inside an optically dense measurement volume. BI utilizes visible light produced by commercially available laser sources, and may be optimized to suit a wide variety of spray condi-

*Corresponding author

tions. With BI, it is possible to acquire breakup information from dense regions of the spray, thereby enabling fully effective spray characterization.

A detailed description of the ballistic imaging instrument used in this work can be found elsewhere [1]. In brief, when light passes through a highly turbid medium, a number of photons pass straight through without scattering. These relatively few photons are termed "ballistic". Since they travel the shortest path, they exit first. A second somewhat larger group is made up of "snake" photons which are scattered once or possibly several times but manage, to a large extent, to retain their original direction of propagation. These photons exit the medium traveling in the same direction as the input light with a larger solid angle than the ballistic photons. Since they travel a larger distance, they exit just after the ballistic photons. Photons that have undergone multiple scattering events, termed diffuse photons, are the most numerous in materials with high extinction coefficients. These photons are scattered into a very large solid angle (4π Sr), and they exit last. The undisturbed path taken by ballistic photons allows the retention of image information regarding structures that may be embedded within the turbid medium. If they are collected by a line-of-sight optical arrangement, the ballistic photons can provide a diffraction-limited shadowgram-type image of these structures. Unfortunately, in most highly scattering environments the number of transmitted ballistic photons is often insufficient to provide the necessary signal-to-noise ratio to form an image in a single-shot format. In such a case, snake photons, together with ballistic photons, can be used for imaging with little degradation in resolution. The problem of obtaining a high-resolution image through highly turbid media is thus a matter of separating and eliminating diffuse light from the ballistic and snake light which retains high-fidelity image information [2]. This can be done by using discrimination methods that make use of the properties of the transmitted light [3]. The BI instrument in this work selects photons based on their propagation direction, polarization, and exit time, using collection optics, crossed Glan-polarizers, and an optical Kerr-effect shutter.

Ballistic Imaging Advantages

When imaging through a measurement volume that exhibits very little scattering, BI yields roughly the same information as a conventional shadowgram [4]. However, when scattered light begins to affect image quality, the differences are quite apparent. Fig. 1(a) shows a white-light shadowgram of an aerated water spray taken with an intensified CCD (Princeton Instruments, PI-Max). Here, the gate-time of the intensifier is used to freeze the motion of the spray. Fig. 1(b) shows a time-gated ballistic image of the aerated spray at the same conditions for comparison. A number of factors contribute to the differences exhibited by the images in Fig. 1(a) and 1(b). Among these, the time-resolution of the image collection, the spatial filtering characteristics of the collection optics, and the specific temporal selection of light provided by the time gate are the most important.

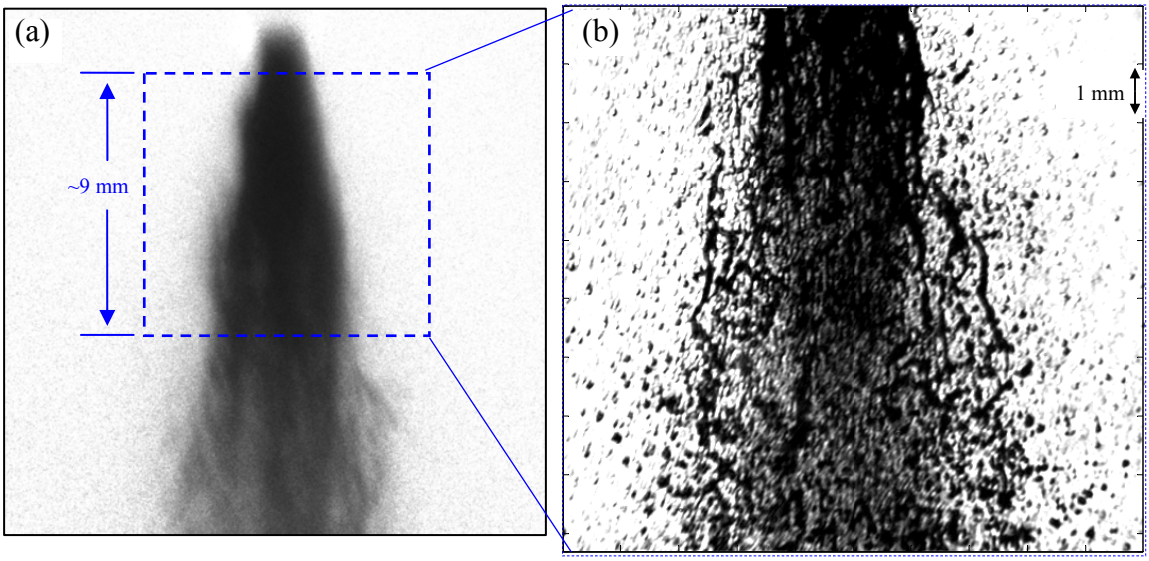

Figure 1. Aerated water spray with 2% gas-to-liquid ratio. (a) shows a focused white-light shadowgram. (b) shows a time-gated ballistic image of the same spray with the ~9 mm field of view indicated by the square inset.

Materials and Methods

Dual images for this study were generated by a time-gated ballistic imaging system specifically designed for transient fuel sprays, applied to a nitrogen aerated water jet issuing into ambient air. The laser source used in this measurement was a specialized ultrafast system capable of generating two 100 fs laser pulses with a user selected time separation. Dual laser pulses with 1 mJ of energy, a pulse width of 100 fs, and a time-separation of 10 μs were used to obtain time-resolved image pairs of the aerated spray.

By employing a fast-framing CMOS camera and the ultrafast laser source described above, consecutive ballistic images with a temporal separation of 10 μs were acquired. This fast detection scheme allows the determination of velocity information from pairs of ballistic images, based on the apparent motion, or "optical flow," of the spatial intensity between corresponding images. For intensity normalized images with a short temporal separation, local image intensity can be assumed to be constant, allowing the optical flow to be written [5]:

$$\frac{\partial E}{\partial x}\frac{dx}{dt}+\frac{\partial E}{\partial y}\frac{dy}{dt}+\frac{\partial E}{\partial t}\approx 0 \qquad (1)$$

where *dx/dt* and *dy/dt* are the components of the motion to be estimated from the image pair, and *E(x, y ,t)* represents the brightness of the image plane at the point (*x, y*).

A variety of methods have been developed to calculate the motion of the spatial intensity in successive images [6, 7, 8]. The results presented here are based on region-matching, using normalized cross-correlation of sub-regions from corresponding image pairs, produced by consecutive pulses of the ultrafast laser source. Prior to analysis, the images are normalized to the measured image background. The image from the first pulse is taken at time t_1; the second pulse produces an image at time, $t_2 = t_1 + 10\mu s$. A set of square image regions are selected from the t_1 image, and cross-correlated with a set of square image regions selected from the t_2 image, yielding *dx/dt* and *dy/dt* velocity components as shown in Eq. 1.

The spray images analyzed in this work are challenging, in the sense that they present large variations in structure and contrast throughout the field of view. Small, well-separated droplets appear on the spray periphery, while the interior of the spray includes large liquid structures and voids with varying amounts of contrast. In order to acquire velocity information throughout the spray, three approaches were applied to select the image regions used to calculate velocity: particle-tracking correlation analysis was applied to obtain velocity for small droplets resolved in the images, conventional non-adaptive grid correlation analysis was applied across the entire field-of-view, and image segmentation with subsequent grid correlation analysis was applied over the resolved fluid features larger than a reasonable size threshold.

For the particle-tracking (PT) approach, a threshold is applied to the background-corrected t_1 image. Connectivity-based image segmentation is then applied to identify image regions. Distinct image regions below a stable droplet size [9] threshold are identified as individual droplets. A square correlation window from the t_1 image is defined to encompass each droplet, and correlated with an appropriately sized search field formed from the t_2 image.

For the grid analysis approach, the entire t_1 image is segmented by a regular grid, such that each square grid element represents a correlation window. Each of these windows is correlated with a search field formed from a t_2 image sub-region centered at the same location.

The third approach is essentially a hybrid of the PT and grid approaches. Large image regions are identified by image segmentation in a manner analogous to the PT approach. A preliminary window is formed for each large region identified in the t_1 image. This preliminary window is then divided into a regular grid, such that each grid element represents a correlation window. These regions are correlated with the sub-regions from the t_2 image centered at the same location.

Results and Discussion

The cross-correlation region matching approach applied here was chosen as a straightforward example to show the feasibility of extracting velocity information from sequential ballistic images, taken with a temporal separation of 10 μs. More refined correlation approaches, for example including additional analysis steps for dynamic window sizing or corrected window offsets, should yield more accurate correlations [10, 11]. The errors involved in image flow analysis such as that employed in this work are explored in the literature [6, 12]. Significant errors are reported for spatial intensity fields without strong features, which serve to form a well-defined cross-correlation peak. Velocity components reported in this work are validated, first by eliminating correlation windows which exhibit very little spatial intensity deviation, and second, by a simple correlation magnitude threshold.

Fig. 3 shows the t_1 image of the aerated spray with 2% gas to liquid ratio (GLR), together with the velocity field calculated from the t_1 and t_2 images. Fig. 4 shows the t_1 image and velocity field of the aerated spray with 10% GLR. Vectors produced by each approach, as explained above, are indicated by color. Green vectors correspond to results produced by the PT method, blue vectors correspond to the grid approach, and red vectors correspond to results from the hybrid method. Here, the vector lengths indicate the displacement from the t_1 image to the t_2 image.

One should note that this is not a planar velocity imaging method like particle-imaging velocimetry (PIV); this is a line-of-sight integrated technique. Hence, the calculated velocity vectors shown in Figs. 3 and 4 appear as expected for the turbulent 3-D spray imaged here. In addition, the velocity indicated by the measured mass-flow at the nozzle exit for the spray in Fig. 4 is ~35 m/s, which compares reasonably well with the mean, ~20 m/s, and range, ~60 m/s, of the calculated velocities for this spray.

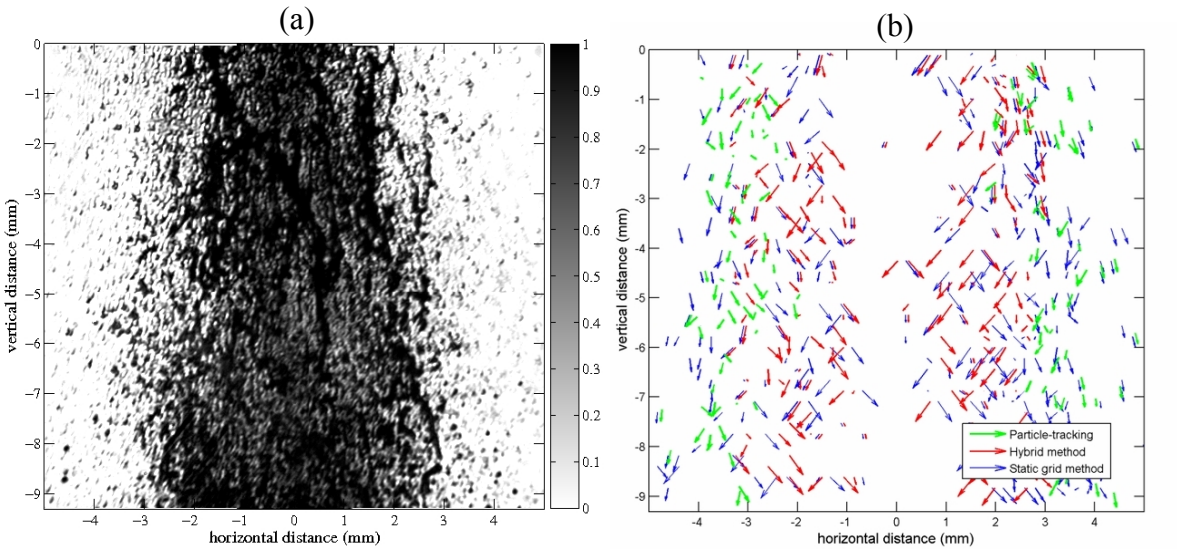

Figure 3. Aerated water spray with 2% gas-to-liquid ratio. (a) shows the time-gated ballistic image taken at time, t_1. (b) shows the velocity field generated from ballistic image pair, taken at times t_1 and t_2.

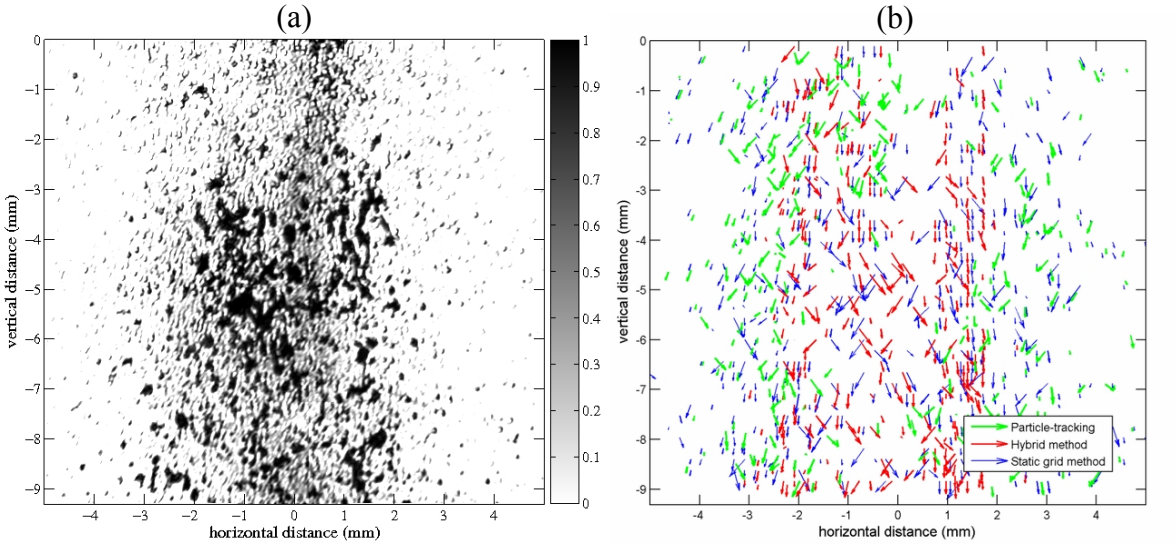

Figure 4. Aerated water spray with 10% gas-to-liquid ratio. (a) shows the time-gated ballistic image taken at time, t_1. (b) shows the velocity field generated from ballistic image pair, taken at times t_1 and t_2.

This procedure produces an adequate number of valid velocity vectors for basic analysis of the complicated flow produced by the spray in this work. However, an in-depth study of this spray would be well-served by a more sophisticated approach which takes advantage the advances made in optical flow and correlation methods, particularly in the fields of particle image velocimetry and machine vision [13].

The results presented here demonstrate that velocity information can be obtained from sequential ballistic images of the near-field of a spray, providing valuable insight into the forces active in primary breakup. The approach presented here opens the way for more advanced analysis of spray breakup dynamics using time-resolved single-shot ballistic imaging.

Acknowledgements

Support for this work was provided by the U.S. Air Force Research Laboratory under contract FA8650-05-C-2522 (Barry Kiel, Technical Monitor), Air Force EOARD grant number FA8655-06-1-3031, and the Air Force Office of Scientific Research (Anne Matsuura, Program Manager). Additional support was provided by CECOST through Swedish Statens Energimyndigheten grant no. 20437-1, and the Swedish Vetenskapsrådet under grant no. 621-2004-5504.

References

1. Linne, M., Paciaroni, M., Berrocal, E., Sedarsky, D., *Proc. Comb. Inst.,* 32:2147-2161 (2009).
2. Berrocal,E., Sedarsky, D., Paciaroni, M., Meglinski, I., Linne, M., *Opt. Express*, submitted.
3. Galland, P., Liang, X.,Wang, L., Breisacher,K., Liou,L., Ho,P., Alfano, R., *Am. Soc. Mech. Eng.*,321:585 (1995).
4. Settles, G., *Schlieren and Shadowgraph Techniques*, Springer, 2001, pp. 148-152.
5. Horn, B., Schunck, B., *Artificial Intelligence*, 17:185-203 (1981).
6. Barron, J., Fleet, D., Beauchemin, S., *Intl. J.Computer Vision*, 1:43-77 (1994).
7. Tokumaru, P., Dimotakis, P., *Exp. Fluids*, 19:1-15 (1995).
8. Bhatti, A., *Stereo Vision*, In-tech, 2008, pp. 335-347.
9. Lefebvre, A., *Atomization and Sprays*, Taylor & Francis, 1989, pp. 34-35.
10. Cowen, E., Monismith, S., *Exp. Fluids*, 22:199-211 (1997).
11. Westerweel, J., Dabiri, D., Gharib, M., *Exp. Fluids*, 23:20-28 (1997).
12. Fielding, J., Long, M., Fielding, G., Komiyama, M., *Appl. Opt.* 40:757 (2001).
13. Raffel, M., Willert, C, Kompenhans, J., *Particle Image Velocimetry: A Practical Guide*, Springer, 1998.